

Terahertz spectroscopy in medical and nutritional applications

G. Salvatella^{a,*}, A. Redo-Sanchez^{b,**}

^aUniversity of Barcelona, Physics Faculty, Microwave and Terahertz Group, 1 martí i franques, 08007 Barcelona (Spain)

^bRensselaer Polytechnic Institute, School of Science, Center for Terahertz Research, 110 8th Street, 12180 Troy NY (USA)

Abstract

THz spectroscopy has recently emerged as a novel technology with several advantages with respect to other spectroscopic techniques, such as real-time data acquisition and non-destructive, non-invasive detection of signatures in medical and food substances. These features have been proven through the use of a THz spectrometer with proper data processing. Several commercially available compounds used in the pharmaceutical and nutritional sector have been analyzed with this technology and have been found to be consistent with the available literature.

Keywords: Terahertz, spectroscopy, pharmaceutical, nutritional

1. Motivation

1.1. The Terahertz Gap

Terahertz (THz) radiation is electromagnetic radiation lying between the microwave and the infrared ranges of the spectrum (usually 0.1–10 THz). Although this frequency band is present in our everyday life, it has remained unexplored until recently due to the lack of efficient and compact THz sources and detectors. The absence of suitable technology for this part of the spectrum led to the designation of the “THz gap”. This technological gap has been lowered down in the last decades thanks to major advances in both optical and microwave technologies, the former down converting higher frequencies and the latter encroaching up from the GHz domain.

The THz range has gained its reputation due to the innumerable physical processes undergone by matter at these frequencies. A multitude of organic compounds and simple molecules do exhibit vibrational and rotational transitions, causing phonon resonance in crystalline structures and bond vibrations in general solids and liquids.

1.2. THz in medical and nutritional applications

Traditionally, quality control in pharmaceutical and food companies has been made after manufacturing by means of subsequent laboratory analysis. To improve consumer safety, several monitoring plans and protocols have been established by the European Commission on the basis of existing legislation [5]. However, regulation systems are costly and entire batches need to be discarded when quality specifications are not fulfilled.

Therefore, the need of analytical technologies that would be implemented throughout the whole manufacturing process encouraged the introduction of spectroscopic techniques such as far- and near-infrared (FIR, NIR) spectroscopy, Raman spectroscopy or nuclear magnetic resonance (NMR) in pharmaceutical companies, as well as microbiological, immunological and chromatographic methods in the food sector.

Such techniques partially solved the problem, but still suffer from being too time-consuming, as the samples usually needs a pre-treat. They are also destructive and invasive, since either the analyzed products require specific preparation or the same analyzing technique is susceptible of affecting the chemical properties of the substances [22]. Withal, the search for novel real-time, non-destructive, non-invasive detection devices stimulated further research in THz technologies, which have shown promising potential in this area.

So far, for instance, pharmaceutical characterization of *polymorphs*¹, detection of contaminants in compounds or even defect scanning in coatings and packages has been demonstrated [2, 10, 17, 34]. Yet there is few information available on the nature of the THz spectra in many compounds, and theoretical models are needed for proper comparison and

*Principal Corresponding Author

**Director

Email addresses: gerard.salvatella@gmail.com (G. Salvatella), aredo@rpi.edu (A. Redo-Sanchez)

¹Polymorphism is the capacity of a substance to crystallize in different structures. Different polymorphs of the same medical substance could cause different effects in their application.



Figure 1: The Mini-Z spectrometer connected to the laser source and a laptop, ready to start measuring.

understanding of the molecular behavior of these substances.

The present work aims to reduce the lack of information by adding analysis of reported and non-reported substances from the medical and nutritional sectors. At the same time, it is intended to prove the efficiency of the first commercially available THz spectrometer featuring portability and real-time data acquisition. Both objectives should bring evidence on the capabilities of this emerging technology.

2. Instrumentation

2.1. Device overview

The device used for the current work is a *Time Domain Spectrometer* and has been manufactured by Zomega Terahertz Corp. The model, Mini-Z Time Domain Spectrometer, was the first real-time, compact and portable spectrometer to be commercialized in the world. With a case size of 27x16x7 cm and 2 kg weight, the Mini-Z operates together with a Ti:sapphire 800 nm laser source and a laptop for data acquisition (figure 1).

The spectrometer is meant to work in the range 1.0 – 4.0 THz. However, measurements have been undertaken in the range 1.0 – 2.0 THz to avoid misinterpretations due to low dynamic ranges. The frequency resolution is around 50 GHz and the scanning rate up to 20 Hz. Dynamic range reaches up to 70dB when operated in transmission mode. The THz emitter consists of a photoconductive antenna, whereas the THz detector is composed of a ZnTe electro-optic crystal and two balanced photodetectors [36].

2.2. Optical elements

A common time domain spectrometer usually works by splitting a laser pulse into two. One of the pulses is converted to THz and passes through the sample, while the other undergoes a controlled path delay. At the end, both pulses interfere and the shape of the longer THz pulse can be “tracked” by the optical pulse upon tuning of the path delay.

The Mini-Z has a similar configuration (v. figure 2). First, the laser source (S) emits a pulse. Recall that the total power of the pulse will be invested in both generation and detection of the THz signal. The pulse is led to a halfwave plate ($\lambda/2$ in the figure) before reaching the beam splitter (BS), in order to adopt the correct polarization.

After the beam splitter, two pulse replicas appear. The “generator” pulse is guided by mirrors to a photoconductive antenna (P), which turns it into a THz pulse. THz beams undergo stronger dispersion than optical, and special aluminum parabolic mirrors (M) as well as high density polyethylene lenses (L) are required for proper focusing into the sample holder.

On the other side, the “probe” pulse (red lines in the figure) is directed to a set of mirrors (m) on top of a moving stage. In the first mirror, the pulse takes a round trip, returning to the beam splitter. Out from the splitter again, it surrounds the stage line (m5, m6 plus a second beam splitter) to reach the second mirror (m) and takes there a two round trip (thanks to the support of m7).

The setting of a *one* round trip at the first mirror and a *two* round trip at the second mirror is of utmost importance. If both mirrors got a one round trip, the moving stage would introduce a zero net delay in the optical path. With the actual asymmetry, a displacement of, say, Δx in the stage, implies a change in the optical path of around $2\Delta x^1$.

Finally, both the THz and the optical pulses come across in an *indium tin oxide* coated mirror (Ito), a material which reflects THz but is mostly transparent at optical frequencies. The Ito mirror aligns both pulses before focusing in a specifically designed quartz lens, fairly absorbant for a wide range of frequencies. The lens has been cut in a crystal orientation such as to exhibit neutral birefringence and focuses the collinear pulses into a 1 mm ZnTe crystal.

The incoming THz pulse induces birefringence inside the ZnTe crystal, which in turn affects the polarization of the optical pulse. A $\lambda/4$ plate then circularly polarizes the pulse. Now a beam splitter known as *Wollaston Prism*

separates the orthogonal polarizations of the pulse and two balanced photodiodes collect the light for comparison and determination of amplitude and phase of the THz electric field. By changing the path delay of the probe pulse with the stage, the THz pulse is “mapped” out, and its frequency components can be extracted after Fourier transformation.

2.3. Performance

The employed spectrometer generates THz pulses through a photoconductive antenna (PCA) composed of low temperature grown gallium arsenide (Lt-GaAs). The emission of THz radiation in a PCA occurs as an electrical switch. Photons of the incident pulse generate electron–hole pairs in the semiconductor, which should be recombined within a subpicosecond time range. For this reason, short carrier life time as well as high carrier mobility and breakdown voltage materials constitute a must in PCA design. Lifetimes of 0.2 ps and carrier mobilities up to 400 cm²/Vs have been reported, which could greatly enhance the performance of the device [14].

The focusing elements in most THz spectrometers consist of collimating lenses made of low-loss polymers such as silicon, polyethylene, teflon and Tsurupica. It is the case of the device used in the current study. However, a more convenient, yet costly, alternative involves off-axis parabolic mirrors coated with aluminum or gold, whose reflectivity is around 99% in both THz and optical ranges. Parabolic mirrors do not produce spherical aberration and point focusing is generally more accurate than in conventional lenses.

The underlying mechanism in the detection process, here called *Electro-optical Sampling* (EO), is the Pockels effect, a second–order nonlinear effect produced when a static electric field induces birefringence in a linear optical medium, which is proportional to the applied field amplitude. In EO sampling, a linearly polarized optical pulse and a THz pulse copropagate through the nonlinear crystal. The birefringence induced by the THz electric field produces a slightly elliptical polarization in the probe pulse. A $\lambda/4$ plate turns the probe polarization into almost circular (but still elliptical). A *Wollaston Prism* then splits the pulse into two orthogonal components (say x and y polarizations), which are collected to a couple of balanced photodetectors. The detectors measure and compute the intensity difference $I_s = I_y - I_x$. The phase delay undergone by the probe pulse over a propagation distance L is

$$\Delta\phi = n_y - n_x \frac{\omega L}{c} = \frac{\omega L}{c} n_O^3 r_{41} E_{THz},$$

where n_O is the optical refractive index, E_{THz} the THz electric field and r_{41} the EO coefficient. The detected intensity in each photodetector and the ultimately measured signal are

$$I_{x,y} = I_0/2(1 \mp \sin \Delta\phi)$$

$$I_s = I_y - I_x = I_0 \Delta\phi = \frac{I_0 \omega L}{c} n_O^3 r_{41} E_{THz},$$

which is proportional to the THz field.

The correct positioning of the $\lambda/4$ plate is also crucial for sensitive detection. In the present device, it has been mounted in a motorized rotatory handler in order to achieve maximum polarization effect while counteracting the polarization instability of the laser source.

Finally, ZnTe crystals show good velocity matching at 800 nm, high transparency at optical and THz frequencies and high EO coefficient ($r_{41} = 4$ pm/V). Field induced birefringence is maximized when the THz field and the probe polarization are parallel to the $[1\bar{1}1]$ axis of a crystal oriented in $\langle 110 \rangle$. Due to transverse optical phonon resonances, ZnTe detection is limited above 4 THz and other nonlinear crystals such as GaSe should be used. Also detection sensitivity increases linearly with crystal thickness, yet detection bandwidth decreases because of velocity mismatch and absorption induced spectral modulation. A trade–off of 1.0 mm has been chosen for the utilized spectrometer.

3. Data analysis

3.1. Time domain, frequency domain

The time domain is a record of what happened to a parameter of a system versus time. It is the traditional way of observing signals. However, when a large signal masks a smaller one, for instance in measurements of noise or distortion, the time domain fails in clearly separating and identifying the small signals. Instead, we convert the signal to the frequency domain, where the frequencies involved remain isolated and easy to see.

¹The correct change in path slightly differs from $2\Delta x$ due to the small angle in the two round trip set of mirrors, as should be visible in figure 2.

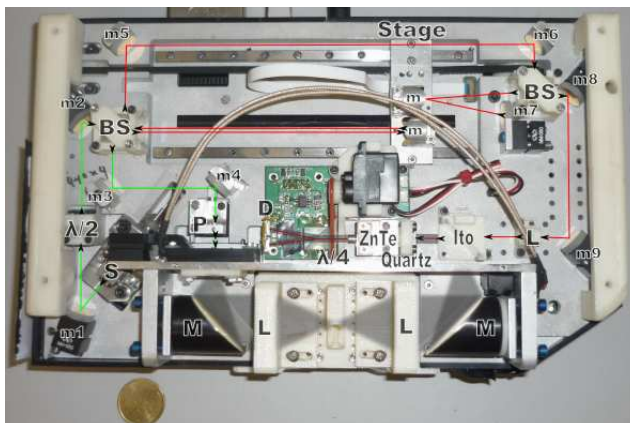


Figure 2: Optical components in the Mini-Z spectrometer. Tags from m1 to m9, m and M indicate mirrors, whereas L indicate lenses. Polarizing plates are represented by $\lambda/2$ and $\lambda/4$ and BS stands for “beam splitter”. S is the laser source, P the photoconductive antenna and D the detector. The remaining components include an indium tin oxide (Ito) mirror, a quartz lens, a ZnTe plate for THz polarization and a moving stage.

In theory, the conversion from time to frequency domain of a signal is achieved through the well known Fourier transform. However, the conventional FT is meant to be used with continuous signals. In real data acquisition, signals need to be sampled in time and a discrete version of FT, called the *Discrete Fourier Transform* (DFT), is then used.

To measure a signal we take samples of it at regular intervals, i.e., with a *sampling period* Δt , during a total *sampling time* T. Reasonably, the lowest measurable frequency in such a sample must be $1/T$. By extension, this is also the smallest difference in frequency, i.e., the *frequency interval* $\Delta f = 1/T$. One should then expect the highest measurable frequency to be $1/\Delta t$ (a wavelength between two time measurements), but two points are insufficient to infer the shape of a wavelength. We are able to deduce the shape of, at most, *half* a wavelength. That is the so called *Nyquist criterion*: the highest measurable frequency in a sampled signal is $1/2\Delta t$.

For a sampled signal consisting of N points, we need N/2 sinusoids to fully describe the signal. Each sinusoid contains *amplitude* and *phase*, which makes a total of N parameters (same as points, as should be). The amplitude A_n and phase ϕ_n of each sinusoid is easily computed with the DFT:

$$\begin{aligned}
 A_n &= \sqrt{a_n^2 + b_n^2} & \phi_n &= -\arctan \frac{b_n}{a_n} \\
 a_n &= \frac{2}{N} \sum_{i=1}^N y(i\Delta t) \cos\left(\frac{2\pi ni}{N}\right) \\
 b_n &= \frac{2}{N} \sum_{i=1}^N y(i\Delta t) \sin\left(\frac{2\pi ni}{N}\right)
 \end{aligned} \tag{3.1}$$

Here $y(i\Delta t)$ is nothing but the value of the signal after i sampling periods (e.g. $i = 3$ is the 3rd sample). Lower n is the *frequency index* and refers to the number of times that the sinusoid fits into the record window (e.g. $n = 1$ refers to a wave that fits one time into the window).

The original sample can be then written, through the inverse DFT transformation, as

$$y(i\Delta t) = \frac{A_0}{2} + \sum_{n=1}^{N/2} A_n \cos(2\pi f_n i\Delta t + \phi_n),$$

where f_n is the value of the frequency, or n times Δf .

3.2. Characterization: aliasing, windowing and averaging

So far, we are able to convert our signal to the frequency domain. Nonetheless, there are a couple of handicaps to be taken into account.

As discussed before, if our signal contains frequencies that lie above the Nyquist frequency, $1/2\Delta t$, the sampling is not accurate enough to resolve them. This means they will not appear in the resulting spectrum as actual frequencies.

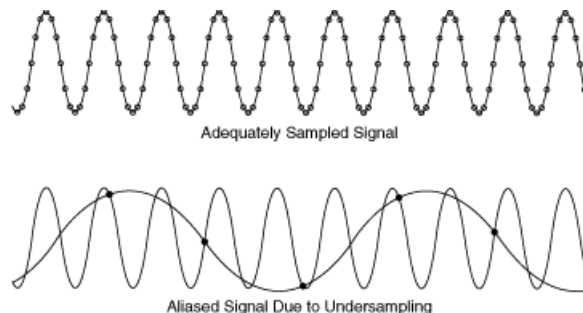


Figure 3: If the sample rate is too low, higher frequencies can be identified as a lower ones, that will add up to the final spectrum. This effect is called *aliasing*.

Instead, the too low sampling rate will identify these higher frequencies as lower ones. These lower, false frequencies are said to be *alias* of the higher, real ones (figure 3). The effect of *aliasing* can then distort the spectrum by adding “ghost” frequencies. The solution to this inconvenient is to use a digital anti-aliasing filter, which suppresses the frequencies above Nyquist’s after the sampling process. Such a filter is included in the electronics of the present device.

There is another feature of the DFT that affects the frequency domain analysis. In fact, when we make a time record of our signal and compute the DFT, the algorithm assumes that such time record is periodic. For instance, if we measure a sine signal, our time record should be of an integer number of wavelengths. Otherwise DFT will incorrectly match the end of the record with its beginning, reconstructing a wrong signal. In the frequency domain, this translates into the appearance of several new frequencies in the spectrum aside from the true one (the sine). This spreading of spectral energy to frequencies other than the desired is known as *leakage*.

For complex signals we cannot have an accurate control of the time records to prevent leakage. Instead, we need to make use of *windowing*. Windows are functions that are zero at the extremes of the interval in which they are defined, but large in the middle. If we convolute such functions with our time record, it automatically turns zero at the extremes and becomes highlighted in the middle. The result: leakage is considerably lowered and even the correct spectrum can be reconstructed². Fortunately, transient signals such as the ones used in TDS-spectrometers (laser pulses) do already have zero values at the extremes and windowing is fairly needed.

Finally, DFT also has to handle noise. To increase the signal-to-noise ratio of a signal, we have used a *linear moving average*. Linear average basically consist of a synchronized average of several time records. If we fix the average number but want our signal to be continuously measured, a moving average will discard the last records while including the newer ones in the average calculation. Other types of averaging such as the exponential moving average, prevent large sudden changes produced by unexpected noise values, but they are also less flexible for spectroscopic measurements (instead, they better suit the needs of many financial average trends).

3.3. Scattering and baseline correction

When measuring absorption in spectroscopic analysis we inevitably measure scattering aswell. In fact, the global process undergone by light that passes through inhomogeneous media is called *extinction*. Extinction includes pure absorption *and* scattering [26]. It is the actual measurement of any spectrometer, although language abuse has incorrectly taken the term absorption for the whole process.

The effect of scattering strongly depends on the ratio between the size of the scattering particles in the media and the wavelength of the incident light. For sizes below 1/10 of the wavelength light is scattered homogeneously over each direction, the resulting intensity changing as $1/\lambda^4$. It is the well known *Rayleigh scattering*. A clear example stands when visible light penetrates in the atmosphere and scatters through the gas particles, leaving blue as the predominant color in the sky. However, for particles above 1/10 of the wavelength, Rayleigh theory breaks down and an exact solution of Maxwell’s equations is then needed. The development of these solutions was first achieved by Gustav Mie and is commonly referred to as *Mie scattering* [26].

In the present work we have dealt with radiation in the range 1–3 THz, i.e. 0.1–0.3 mm. Since particles in the powder used for the preparation of samples lie in this range of sizes, the exhibited scattering has predominantly been of Mie type. Accurate calculations of Mie scattering involve certain knowledge of the microscopic structure of the medium.

²In fact, a convolution of two real time signals translates into a simple product of the respective fourier transforms. One can then get rid of the windowing effect in the frequency domain by means of a division.

Therefore, when coping with spectroscopic measurements, a more *in situ* approach is used for subtracting the scattering effect, namely, the baseline correction.

Fortunately, the scattering pattern can be often differentiated from the pure absorption in that it appears as a long wave signal, also called a trend or *baseline*. For this reason, an experimental way to remove the baseline of a signal entails fitting the signal with a low grade polynomial. The polynomial does not fit the complete signal, but roughly fits the trend. An iterative process called *polynomial fitting with automatic threshold*, suggested in [8], has been used in this study to successively fit the polynomial to the actual baseline with a determined accuracy. The obtained baseline has been then removed from the signal in order to isolate the pure absorption pattern.

The first step of the process has involved fitting an n grade polynomial with the usual least squares method. That is, we have taken a polynomial of the form

$$y = a_0 + a_1x + \dots + a_nx^n$$

and computed the derivatives of the residual (least squares)

$$R^2 = \sum_{i=1}^k [y_i - (a_0 + a_1x_i + \dots + a_nx_i^n)]^2$$

with respect to a_0, a_1, \dots, a_n . Here y_i are the values of our sampled signal at each frequency x_i . Computation of such derivatives form a set of n equations for the constants a_i . The solution for the constants can be written in a simple matrix form. If we take

$$\mathbf{y} = \begin{pmatrix} y_1 \\ y_2 \\ \vdots \\ y_k \end{pmatrix} \quad \mathbf{X} = \begin{pmatrix} 1 & x_1 & \cdots & x_1^n \\ 1 & x_2 & \cdots & x_2^n \\ \vdots & \vdots & \ddots & \vdots \\ 1 & x_k & \cdots & x_k^n \end{pmatrix} \quad \mathbf{a} = \begin{pmatrix} a_0 \\ a_1 \\ \vdots \\ a_n \end{pmatrix},$$

then we can put

$$\mathbf{a} = (\mathbf{X}^T \mathbf{X})^{-1} \mathbf{X}^T \mathbf{y}$$

as the constants that produce the polynomial with the minimum square deviation from the data. The polynomial itself is simply

$$\mathbf{b} = \mathbf{X} (\mathbf{X}^T \mathbf{X})^{-1} \mathbf{X}^T \mathbf{y}$$

In other words, \mathbf{b} is now a rough estimate of the trend of the signal, \mathbf{y} .

The second step has entailed polishing up our estimate. In order to do that, we have compared the values b_i with the values of the actual signal, y_i , near the peak regions. The parts of the actual signal with values greater than the trend estimate have been cut off (i.e. if $b_i > y_i$ then set $y_i = b_i$). The tuned signal contained then lesser peaks and revealed the baseline. A new polynomial could be fitted, which would more precisely describe the baseline, and the same polishing process should be followed again until a certain accuracy. Eventually, this iterative method identifies the baseline, which can be removed from the original signal to subtract the scattering pattern.

4. Methodology

4.1. Sample preparation

Medical substances have been purchased in tablet form from a drugstore and are commercialized throughout the country. Saccharides have been obtained from Sigma-Aldrich Inc., whereas riboflavin and doxycycline have been taken from laboratories in the Polytechnic University of Catalonia (UPC).

Samples have been prepared in a pellet form using a matrix of high density polyethylene (PE) powder. Typically, the total weight of the sample is 150 mg with an amount of substance between 5 mg and 30 mg. The mixture of sample and PE has been grinded in a porcelain mortar and pressed with a hydraulic press at 2 tones. The total thickness of the pellet is about 2 mm.

4.2. Measurement conditions

Measurements have been made under the following conditions.

First, the spectrometer has been purged with nitrogen gas in order to minimize the effects of water vapor, which is highly absorbant in the THz range (figure 4). Purging has entailed connecting a flexible plastic tube to a corresponding hole in the spectrometer. Nitrogen gas has been injected through the tube, displacing the air inside the spectrometer, hence decreasing humidity down to a 2%.

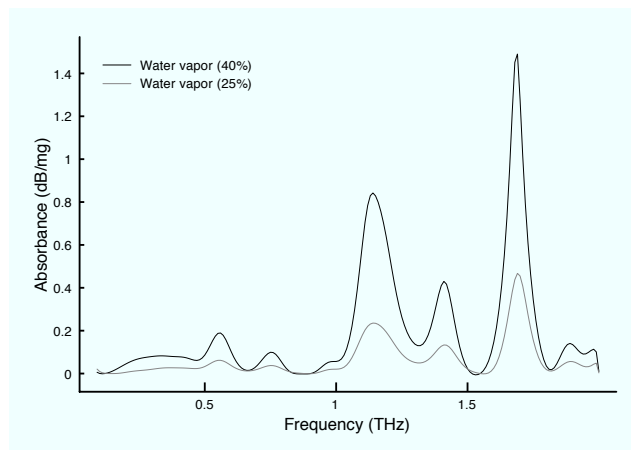


Figure 4: Absorption spectra of water vapor (25% and 40% humidity) between 0.1 and 1.8 THz. The spectrometer has been purged with nitrogen to establish a reference level (2% humidity) and subsequent measurements at 25% and 40% humidity have been taken. Observed peaks lie at 0.56, 0.75, 1.14, 1.41 and 1.69 THz

Second, a measure of the noise level has been obtained by stopping the radiation beam with a metallic plate. The incident beam not reaching the detector, the measured signal only contains proper noise. Noise level allows determining the *dynamic range* of the device against frequency, i.e., the difference (in dB) between the intensity of the measured signal and the noise signal.

Third, pure high density polyethylene pellets have been used as a reference, upon which data of the samples has been taken¹. This procedure suppresses any possible absorption features of the polyethylene, used in the preparation of the samples.

Finally, 10 measurements of each sample have been undertaken. In each repetition, the sample pellet has been extracted and reinserted in the sampleholder. By averaging the spectra, systematic errors produced by wrong positioning, as well as present heterogeneities in the sample, have been minimized.

5. Results and discussion

5.1. Medical substances

Adiro and Aspirin, from the same manufacturer, contain acetylsalicylic acid in 74.1% and 84.0% respectively. The amount of active substance analyzed has been 30mg. Mean excipients are starch and cellulose, which are known to be mostly featureless in the THz range [19, 32, 22]. A potential peak has been found around 1.01–1.04 THz. Minor features in figure 5a and 5b are not reproducible, its major causes being inhomogeneities in the sample and misinterpretations of the baseline correction algorithm.

Literature is available for aspirin spectra in the THz range [11, 13, 30]. However, in most cases either peak positions are not specified, or measurements have been made at low temperatures. Nonetheless, the observed spectra at [13, 30] suggest a weak feature precisely around 1 THz, which could reproduce the aforesaid.

Finally, it should be mentioned that, at the moment, only one stable polymorph of aspirin is known at room temperature [27]. Therefore, a criterion for polymorphism comparison cannot be established.

Polaramine and Polaramine Repetabs, two antihistamines from the same manufacturer, include dexchlorfeniramin maleato as the active substance. Only 5mg of the substance have been used in the sample, since each tablet contains it in a 2.4%. Both samples have shown three clear absorption peaks at 0.53 THz, 1.19 THz and 1.38 THz whose amplitude is conspicuously greater than the rest of the samples. Even so, it has been considered that the peaks are associated to one of the existing excipients, α -lactose, due to the strong coincidence with the features published in [31, 3, 16, 29].

Remarkably, Saito et al. [21] have computed the vibrational and rotational modes for the α -lactose molecule through *Periodic Density Functional Theory*, a numerical method based in the Hartree-Fock equations. They have claimed one rotational mode at 0.525 THz, two translational modes at 0.993 THz, 1.110 THz, and a vibrational mode at 1.320 THz, among others.

¹The TDS-spectrometer registers, as said, data in time domain and converts it to frequency domain. A reference spectrum should be established manually, over which the spectrometer will determine the absorbance of the sample.

As for polymorphism, Kirk et al. [12] concluded four forms for lactose. α -lactose monohydrate, or $L\alpha H_2O$, is the most usual, present in milk and commercialized as an ingredient of most nutritional products. It is the most stable form in dissolution below 120°C, and it is then likely to be the only present form in medical excipients. The remaining are dehydrated forms of lactose, namely, β -lactose, $L\beta$, stable α -lactose, $L\alpha_S$, and unstable, hygroscopic α -lactose, $L\alpha_H$. All three forms are obtained directly from the monohydrated form through different thermal techniques [7, 12].

Besides the three referenced peaks, Xiao-jing et al. [33] have found similar features at 1.21 THz and 1.38 THz for $L\beta$. On the other hand, Zeitler et al. [35] have reported peaks at 0.90 THz, 1.08 THz and 1.42 THz for $L\alpha_S$. Still the evidence of differences in THz spectra of the lactose forms remains an open topic.

Ibuprofen samples have been examined through Ibuprofen Cuve and Neobrufen, 75.5% and 50.7%, in quantities of 30mg (figure 5c, 5d). Additionally, a sample of pure ibuprofen, not shown in figure 5, has also been analyzed for comparison. A reproducible absorption mark has been detected around 1.03–1.05THz. Two minor marks around 0.53 THz and 1.20 THz reveal the presence of α -lactose as an excipient in both cases, with a higher concentration in Neobrufen. Studies have been undertaken on quality control proof-of-concept using ibuprofen tablets [6], however no spectroscopic measurements have been found in the public literature.

Ibuprofen is currently available in racemic mixture form, i.e., an aggregate of the enantiomers S(+)-ibuprofen and S(-)-ibuprofen in equal shares, where S(+) is the active principle in the medical substance. Dudognon et al. [4] sustain that, despite demonstration of ibuprofen crystals with different morphologies (crystal size, surface, etc) has been suggested, such crystal structures are in general isomorphic and genuine polymorphism should be discarded, albeit the reported in their publication. In any case, the supposed polymorphs of ibuprofen are mostly synthesized at cryogenic temperatures and unlikely to be present in medical substances at room temperature. No evidence of polymorphism has been inferred from the obtained spectra of ibuprofen samples.

5.2. Nutritional substances

Riboflavin, also known as vitamin B2, is an important micronutrient involved in several metabolic processes, present in many manufactured food products. A 30mg sample of pure riboflavin has been analyzed. A double peak at 1.04 THz, 1.18 THz as well as a tertiary feature at 1.51 THz have been observed (figure 5i). Takahashi et al. [23], who have also measured riboflavin at room temperature, locate similar marks at 1.03 THz, 1.18 THz and 1.52 THz, whereas Gorenflo et al. [9] show a spectrum with an analogous double peak pattern around the same frequencies (although experimental values have not been specified). Fortunately, riboflavin powder has an unexpected small particle size, which allows highly homogeneous preparation of the samples and prevents from scattering effects. Consequently, the absorption profile has been found to be generally more stable than in other samples.

Glucose, an ubiquitous monosaccharide in most living organisms, is considered to be the main energy source for cells. Upon examination of a 30mg sample of D-glucose, a single feature at 1.41 THz has been reproduced throughout (figure 5g). Although saturation in the absorption spectrum has been reached after 1.6 THz due to strong scattering of the glucose crystals, Liu et al. [15], who also measured D-glucose monohydrate, report an analogous mark at 1.44 THz, however not exhibited in the hydrated form. figure 5g is also consistent with previous experiments [25, 28, 33].

In a similar way, sucrose, the basic component of commercial sugar, is structured as a disaccharide, formed by a glucose and a fructose. Analysis of a 30mg sample of crystalline sucrose powder has revealed an absorption mark at 1.42 THz (strong scattering of sucrose crystals has also produced saturation above 1.6 THz, as the lack of data in figure 5h brings out). It has been suggested that such feature proves the presence of glucose in sugar, since reported features of fructose are out of this frequency [24, 28]. If so, this fact could demonstrate the potential of THz spectroscopy in distinguishing the components of a substance. Furthermore, the displayed absorption marks are in agreement with what reported in [20, 28].

It is noteworthy to recall that sucrose derived from commercial sugar only crystallizes in the anhydrous form and is found in a single isomer [1]. Therefore, no differentiation in polymorphism need to be accounted for.

Finally, a 30mg sample of doxycycline, an antibiotic with broad applications (including malaria treatment and feed sterilization [18]), has been studied. Three features, one at 0.90 THz and a double peak at 1.21 THz and 1.58 THz, have been clearly identified, with absorption amplitudes higher than in previous samples (notice the scale change in figure 5j). No references in the published literature have been found for doxycycline in the THz range.

6. Conclusions

After understanding and enhancement of the spectrometer functioning and proper data processing, the efficiency and feasibility of THz spectroscopy for medical and nutritional applications in real-time, non-invasive measurements has been proved. Suitable absorption spectra of broadly used medical and food substances has been obtained. Reported signatures in the available literature were in agreement with the exhibited, while the remaining would require confirmation from other sources.

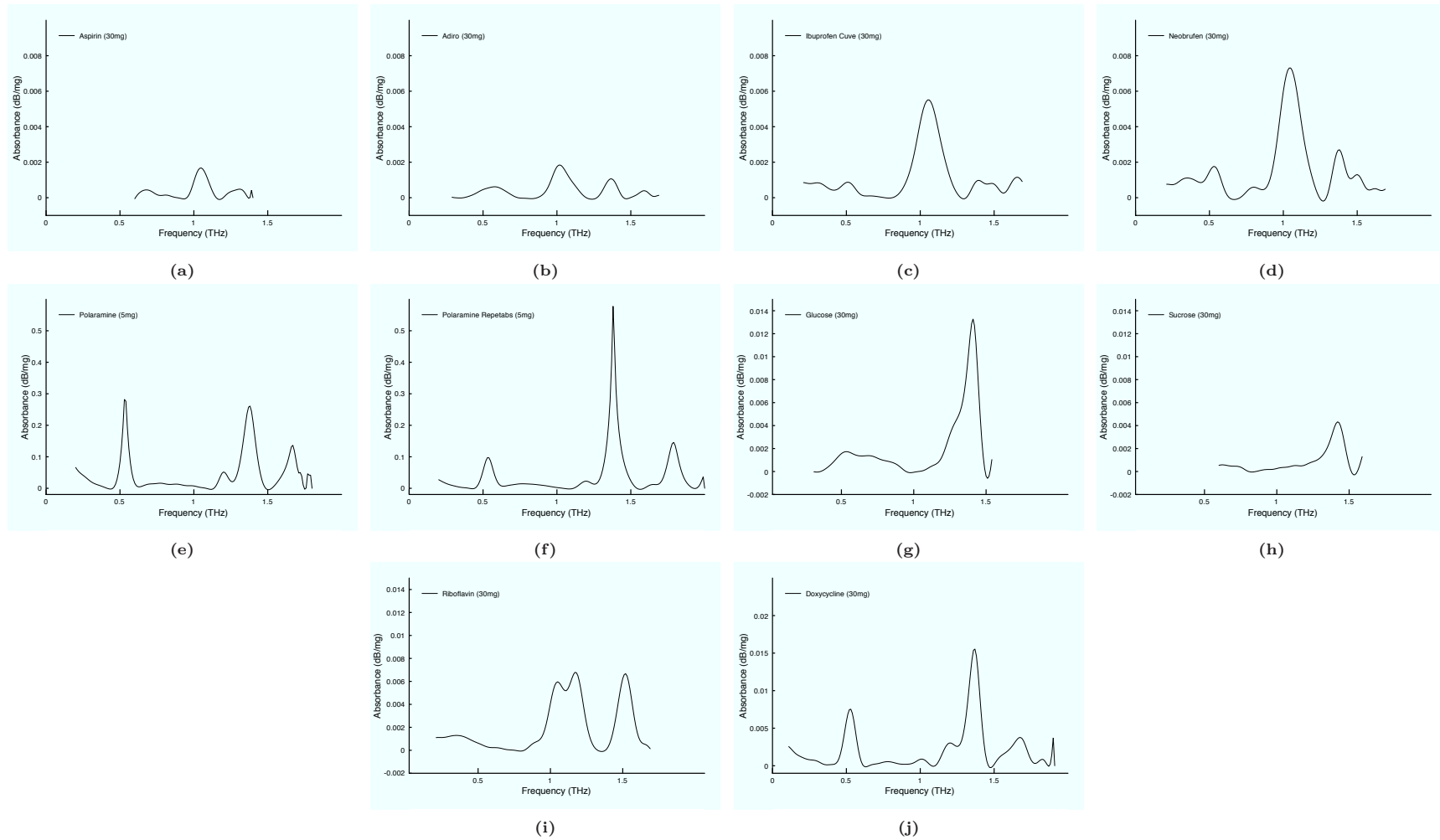


Figure 5: Analyzed medical and nutritional substances. (5a) Aspirin and (5b) Adiro contain acetylsalicylic acid; (5c) Ibuprofen Cuve and (5d) Neobrufen are a generic and commercial brands for ibuprofen; (5e) Polaramine and (5f) Polaramine Repetabs (long effect tablets) contain dexchlorfeniramin maleato as active substance, but the present features are considered to belong to one of its excipients, α -lactose. Notice the change in scale for the last two figures. (5g) glucose, (5h) sucrose, made of a glucose and a fructose, (5i) riboflavin or vitamin B2 and (5j) doxycycline, a broadly used antibiotic.

References

- [1] Beevers, C., McDonald, T., Robertson, J., 1952. The crystal structure of sucrose. *Acta Crystallographica Section B: Structural Crystallography and Crystal Chemistry* 5, 689–690.
- [2] Brandt, N., Chikishev, A., Kargovsky, A., Nazarov, M., Parashchuk, O., Sapozhnikov, D., Smirnova, I., Shkurinov, A., Sumbatyan, N., 2008. Terahertz time-domain and raman spectroscopy of the sulfur-containing peptide dimers: Low-frequency markers of disulfide bridges. *Vibrational Spectroscopy* 47 (1), 53–58.
- [3] Brown, E., Bjarnason, J., Fedor, A., Korter, T., 2007. On the strong and narrow absorption signature in lactose at 0.53 thz. *Applied Physics Letters* 90, 061908.
- [4] Dudognon, E., Danède, F., Descamps, M., Correia, N., 2008. Evidence for a new crystalline phase of racemic ibuprofen. *Pharmaceutical research* 25 (12), 2853–2858.
- [5] European Commission, July 2010. European commission. on the implementation of national residue monitoring plans in the member states in 2008.
URL <http://ec.europa.eu/food/food/chemicalsafety/residues>
- [6] Fitzgerald, A., Cole, B., Taday, P., 2005. Nondestructive analysis of tablet coating thicknesses using terahertz pulsed imaging. *Journal of pharmaceutical sciences* 94 (1), 177–183.
- [7] Fox, P., 1992. *Advanced Dairy Chemistry: Lactose, water, salts and vitamins*. Springer U.S.
- [8] Gan, F., Ruan, G., Mo, J., May 2006. Baseline correction by improved iterative polynomial fitting with automatic threshold. *Chemometrics and Intelligent Laboratory Systems* 82 (1-2), 59–65.
- [9] Gorenflo, S., Hinkov, I., Lambrecht, A., Fischer, B., Hoffmann, M., Helm, H., Jepsen, P., 2005. Low-power terahertz time-domain spectroscopy with optimized electro-optical detection. *Technisches Messen* 72 (7/8), 430.
- [10] Jordens, C., Koch, M., 2008. Detection of foreign bodies in chocolate with pulsed terahertz spectroscopy. *Optical engineering* 47 (3).
- [11] Kawase, K., Ogawa, Y., Watanabe, Y., Inoue, H., 2003. Non-destructive terahertz imaging of illicit drugs using spectral fingerprints. *Opt. Express* 11 (20), 2549–2554.
- [12] Kirk, J., Dann, S., Blatchford, C., 2007. Lactose: A definitive guide to polymorph determination. *International journal of pharmaceutics* 334 (1-2), 103–114.
- [13] Laman, N., Harsha, S., Grischkowsky, D., 2008. Narrow-line waveguide terahertz time-domain spectroscopy of aspirin and aspirin precursors. *Applied spectroscopy* 62 (3), 319–326.
- [14] Lee, Y.-S., 2009. *Principles of terahertz science and technology*, 1st Edition. Springer.
- [15] Liu, H., Chen, Y., Zhang, X., 2007. Characterization of anhydrous and hydrated pharmaceutical materials with thz time-domain spectroscopy. *Journal of pharmaceutical sciences* 96 (4), 927.
- [16] Logan, R., Demers, J., 2009. Photonic integration improves heterodyne photomixing terahertz sources. *Laser Focus World* 45 (9).
- [17] Morita, Y., Dobroiu, A., Otani, C., Kawase, K., 2005. A real-time inspection system using a terahertz technique to detect microleak defects in the seal of flexible plastic packages. *Journal of Food Protection* 68 (4), 833–837.
- [18] National Library of Medicine, September 2010. Anhydrous doxycycline.
URL <http://druginfo.nlm.nih.gov/drugportal>
- [19] Palermo, R., Cogdill, R., Short, S., Drennen III, J., Taday, P., 2008. Density mapping and chemical component calibration development of four-component compacts via terahertz pulsed imaging. *Journal of pharmaceutical and biomedical analysis* 46 (1), 36–44.
- [20] Rungswang, R., Ueno, Y., Tomita, I., Ajito, K., 2006. Terahertz notch filter using intermolecular hydrogen bonds in a sucrose crystal. *Opt. Express* 14, 5765–5772.
- [21] Saito, S., Inerbaev, T., Mizuseki, H., Igarashi, N., Ryunosuke, N., Kawazoe, Y., 2006. First principles calculation of terahertz vibrational modes of a disaccharide monohydrate crystal of lactose. *Japanese Journal of Applied Physics* 45 (43), L1156–L1158.
- [22] Taday, P., 2004. Applications of terahertz spectroscopy to pharmaceutical sciences. *Philosophical Transactions A* 362 (1815), 351.
- [23] Takahashi, M., Ishikawa, Y., Nishizawa, J., Ito, H., 2005. Low-frequency vibrational modes of riboflavin and related compounds. *Chemical Physics Letters* 401 (4-6), 475–482.
- [24] Upadhyaya, P., Shen, Y., Davies, A., Linfield, E., 2004. Far-infrared vibrational modes of polycrystalline saccharides. *Vibrational Spectroscopy* 35 (1-2), 139–143.
- [25] Upadhyaya, P., Shen, Y., Davies, A., Linfield, E., October 2004. Terahertz time-domain spectroscopy of glucose and uric acid. *Journal of Biological Physics*, 117–121.
- [26] Van De Hulst, H., 1981. *Light scattering by small particles*, 1st Edition. Dover Publications, Inc.
- [27] Vishweshwar, P., McMahon, J., Oliveira, M., Peterson, M., Zaworotko, M., November 2005. The predictably elusive form ii of aspirin. *J. Am. Chem. Soc* 127 (48), 16802–16803.
- [28] Walther, M., Fischer, B., Uhd Jepsen, P., 2003. Noncovalent intermolecular forces in polycrystalline and amorphous saccharides in the far infrared. *Chemical Physics* 288 (2-3), 261–268.
- [29] Walther, M., Freeman, M., Hegmann, F., 2005. Metal-wire terahertz time-domain spectroscopy. *Applied Physics Letters* 87, 261107.
- [30] Walther, M., Plochocka, P., Fischer, B., Helm, H., Uhd Jepsen, P., 2002. Collective vibrational modes in biological molecules investigated by terahertz time-domain spectroscopy. *Biopolymers (Biospectroscopy)* 67 (4-5), 310–313.
- [31] Withayachumnankul, W., Fischer, B., Abbott, D., 2008. Material thickness optimization for transmission-mode terahertz time-domain spectroscopy. *Opt. Express* 16, 7382–7396.
- [32] Wu, H., Heilweil, E., Hussain, A., Khan, M., 2008. Process analytical technology (pat): Quantification approaches in terahertz spectroscopy for pharmaceutical application. *Journal of pharmaceutical sciences* 97 (2), 970–984.
- [33] Xiao-jing, M., Hong-wei, Z., Gui-feng, L., Te, J., Zeng-yan, Z., Bin, D., November 2009. Qualitative and quantitative analyses of some saccharides by thz-tds. *Spectroscopy and spectroscopic analysis* 29 (11), 2885–2888.
- [34] Yang, L., Sun, H., Weng, S., Zhao, K., Zhang, L., Zhao, G., Wang, Y., Xu, Y., Lu, X., Zhang, C., et al., 2008. Terahertz absorption spectra of some saccharides and their metal complexes. *Spectrochimica Acta Part A: Molecular and Biomolecular Spectroscopy* 69 (1), 160–166.
- [35] Zeitler, J., Kogermann, K., Rantanen, J., Rades, T., Taday, P., Pepper, M., Aaltonen, J., Strachan, C., 2007. Drug hydrate systems and dehydration processes studied by terahertz pulsed spectroscopy. *International journal of pharmaceutics* 334 (1-2), 78–84.
- [36] Omega Corp., August 2010. Mini-z terahertz time domain spectrometer.
URL <http://www.omega-terahertz.com/products/index.html>